Published in
Applied Physics B: Lasers and Optics 103, issue 4, 967-970, 2010
which should be used for any reference to this work

CO_2 isotope sensor using a broadband infrared source, a spectrally narrow 4.4 μm quantum cascade detector, and a Fourier spectrometer

D. Hofstetter · J. Di Francesco · L. Hvozdara · H.-P. Herzig · M. Beck

Abstract We report a prototype CO_2 gas sensor based on a simple blackbody infrared source and a spectrally narrow quantum cascade detector (QCD). The detector absorption spectrum is centered at 2260 cm^{-1} (4.4 μm) and has a full width at half maximum of 200 cm^{-1} (25 meV). It covers strong absorption bands of two spectrally overlapping CO_2 isotopomers, namely the P-branch of $^{12}CO_2$ and the R-branch of $^{13}CO_2$. Acquisition of the spectral information and data treatment were performed in a Fourier transform infrared (FTIR) spectrometer. By flushing its sample compartment either with nitrogen, dry fresh air, ambient air, or human breath, we were able to determine CO_2 concentrations corresponding to the different gas mixtures. A detection limit of 500 ppb was obtained in these experiments.

1 Introduction

Semiconductor-based compact gas sensors using optical absorption can be realized with different technologies. Thanks to the recent development of room temperature operated continuous wave mid-infrared lasers such as the quantum cascade laser (QCL), substances being relevant for atmospheric pollution, process control, and environmental sensing can now be detected at high resolution [1, 2]. Besides a good signal to noise ratio and thus a low detection limit, the excellent wavelength selectivity of QCLs allows a straight-forward discrimination of different isotopomers. As a prominent example of the medical area, non-invasive ^{13}C-breath tests are performed, where human enzyme activities, organ functions, and transport processes can be assessed [3]. Such tests detect a possible *Helicobacter pylori* infection of the stomach or the duodenum; in addition, they can be easily performed and have a high patient acceptance. Unfortunately, the elevated cost of QCLs is still a major issue, which so far prevented them from providing a real breakthrough in medical sensing. Alternatively, breath tests using different types of spectroscopy involving several N_2O and CO isotopes can be carried out. Such techniques have been developed extensively by M. Murtz et al. [4, 5]. Therefore, the use of a highly sensitive and spectrally narrow detector along with a broadband infrared light source could be an attractive alternative to laser-based spectroscopy. A perfectly suitable device for such applications is the photovoltaic quantum cascade detector (QCD) [6]. For a selected wavelength range determined by the detector's response curve, this method results in both a good spectral resolution and a high sensitivity. Ideally, the QCD is constructed as a linear pixel array, and will be combined with a miniaturized grating spectrometer. It can be fabricated using standard III–V-semiconductor technology and custom-designed with up to 1024 elements. For the prototype measurements presented in this paper, where only a single pixel detector was available, the spectral information was obtained thanks to a Fourier transform infrared spectrometer (FTIR). In a later

D. Hofstetter (✉) · J. Di Francesco
Institute of Physics, University of Neuchâtel,
51 Avenue de Bellevaux, 2009 Neuchâtel, Switzerland
e-mail: Daniel.hofstetter@unine.ch
Fax: +41-32-7182901

L. Hvozdara · H.-P. Herzig
Optics and Photonics Technology Laboratory,
Institute of Microtechnology, EPFL, A.-L. Breguet 2,
2000 Neuchâtel, Switzerland

M. Beck
Quantum Optoelectronics Group, Institute of Quantum
Electronics, ETHZ, Wolfgang-Pauli-Strasse 16, 8093 Zurich,
Switzerland

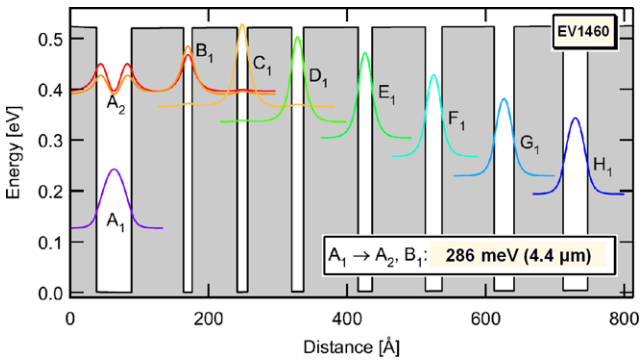

Fig. 1 Schematic representation of one active region period of a typical QCD showing relevant wavefunctions and saw-tooth potential. The device presented in this article has a transition energy of 286 meV (4.4 µm)

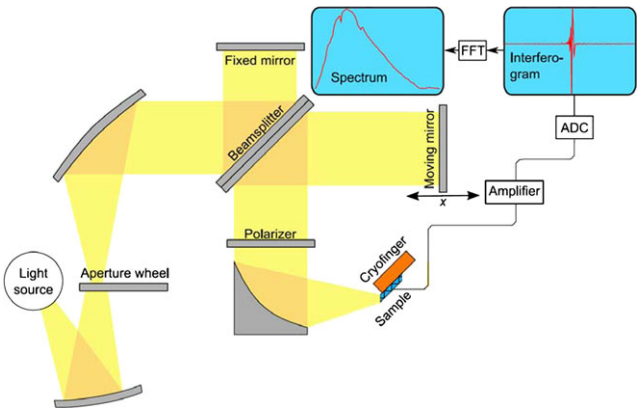

Fig. 2 Schematic representation of the FTIR-based setup for the sensor characterization described in this article. The light source is in this case a blackbody source at 1460 K

version, we envisage the use of a linear array of QCDs along with a much simpler and well-adapted grating spectrometer.

2 Fabrication

The QCD used in this experiment had an active surface of 200×200 µm^2. Epitaxial growth of this device was performed via molecular beam epitaxy of multiple InGaAs/InAlAs layers on an InP substrate. One active region period is depicted in Fig. 1. It comprises a Si-doped (1.5×10^{18} cm^{-3}) main quantum well with a thickness of 5.2 nm, and an extraction region consisting of 7 additional quantum wells with increasing thickness. Under absorption of a photon with $\Delta E_{12} = 286$ meV, electrons undergo first an optical transition from the ground state A_1 into the first excited state A_2 of the main well. From there, they perform a resonant tunneling transition into the uppermost quantized state of the extraction region (B_1) and then scatter down to the ground state of the following period A_1'. A QCD typically counts 20 to 30 such active region periods which are sandwiched between two highly-doped contact layers. The fabrication procedure was based on chemical wet etching of mesa structures in order to access the lower contact layer of the detector. Ti/Ge/Au/Ag/Au (1.5/12/27/50/300 nm) contacts are then evaporated on both bottom and top contact layers. Finally, contact annealing, polishing of a 45° wedge or etching of a diffraction grating for efficient optical coupling, and device mounting on a copper holder completed the processing. Details on the fabrication can be found in Ref. [6].

3 Experimental setup and results

3.1 Experimental setup and QCD characteristics

For the measurement of both responsivity and CO_2 absorption curves, an experimental setup as shown in Fig. 2 was used. On the emitter side, it consisted of an FTIR spectrometer (Bruker IFS-66) and its internal glow-bar infrared source. The latter can be regarded as a nearly ideal blackbody emitter at 1460 K with a size of 3 mm in diameter. Its output was focused onto the 45° facet of the QCD using a single parabolic mirror with a focal distance of 4 inches. The QCD was mounted in a liquid nitrogen flow cryostat and stabilized at temperatures ranging from 150 K to 300 K. The purely photovoltaic QCD signal was amplified via a low-noise current amplifier (SR570) with a gain of 0.2 µA/V, bandpass-filtered between 300 Hz and 10 kHz, and fed back to the external detector port of the FTIR. Since the characteristics of the FTIR's glow-bar light source were calibrated previously, one could exactly determine the responsivity of the QCD. A series of response curves measured between 150 K and 300 K is presented in Fig. 3. Each measurement shown is the result of 200 averaged rapid scans. Typical responsivity values for such a QCD are on the order of 5 mA/W at 300 K and 9 mA/W at 175 K. Since there is no dark current noise, the dominant noise mechanism of the device is Johnson noise. At an operating temperature of 175 K, which resulted in maximum performance, we observed a device resistance of 175 kΩ and therefore a detectivity of 5×10^8 jones. It is important to note that temperatures around 200 K can be maintained by thermo-electric coolers, and that they do not require the use of liquid nitrogen cooling systems. For the purpose of comparison, we give here the detectivity values for commercial detectors at similar temperatures. Laser Components, for instance, sells a broad band photodetective PbSe sensor at 2300 cm^{-1} and 243 K with a detectivity of 3×10^{10} jones (SCD-15 series). Experience has shown that a spectrally narrow detector could still be somewhat better, on the order of 5×10^{10} jones. At the same time, Hamamatsu markets a two-stage Peltier photoconductive broad band InSb detector (P6606 series) at 243 K with a detectivity of 3×10^9 jones. This is to be compared with our value of 5×10^8 jones for a photovoltaic QCD at 175 K. However,

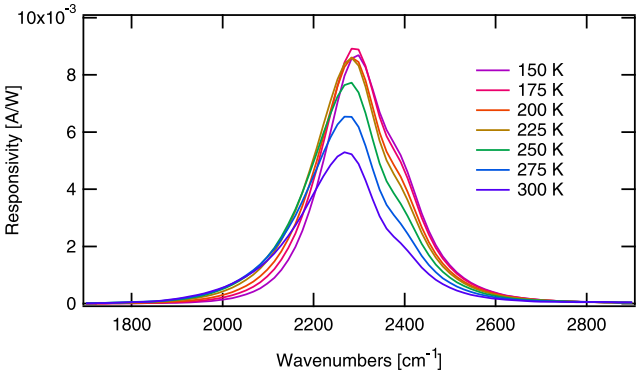

Fig. 3 Responsivity curves of a 4.4 µm QCD as a function of temperature. The little bump around 2330 cm^{-1} is due to CO_2 absorption bands

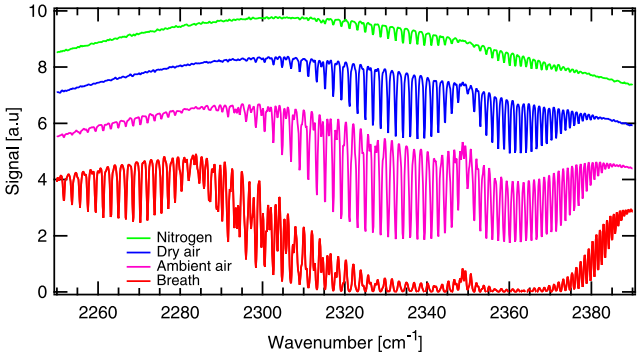

Fig. 4 Comparison between different purge conditions. The *green*, *blue*, and *violet curves* correspond to CO_2-concentrations of 10 ppm, 100 ppm, and 340 ppm, respectively. The *red curve* is for a much higher concentration, namely 5000 ppm. The resolution of these measurements was 0.25 cm^{-1}

it must be noted that neither PbSe nor InSb based detectors lend themselves easily for fabrication as linear arrays. For a QCD, this is straight-forward and will certainly be the natural next step to go.

3.2 Absorption of CO_2 isotopomers

Since CO_2 is at its present planetary concentration of 340 ppm an important green-house gas in earth's atmosphere, it can be easily measured using the prototype sensor described in this article. The main absorption bands are due to the asymmetrical stretch vibration of the CO_2 molecule. More particularly, the band centered around 2360 cm^{-1} is called the R-branch, while the one around 2330 cm^{-1} is the P-branch. In the following experiments, absorption measurements have been carried out under different experimental conditions. To illustrate this, we show in Fig. 4 a comparison between measurements with a pure nitrogen purge, a dry fresh air purge, an ambient air purge, and a sample of human breath. In all experiments, the 30 cm long optical path between the FTIR and the QCD served as absorption cell. In order to maintain a constant gas concentration along this path, a tubular protection was mounted around the beam. As Fig. 4 shows, there is a substantial signal change between the different measurements. For clarity, three out of four curves have been vertically displaced by 1.5 a.u. (ambient air), 3.0 a.u. (dry fresh air), and 4.5 a.u. (nitrogen). Purging the FTIR for 10 minutes with pure N_2 led to a small CO_2 absorption of only about 10% of the peak value (green trace). A simulated spectrum based on the HITRAN database indicated that the concentration was in this case 10 ppm [7]. Given the observed signal to noise ratio of the absorption curve, a detection limit of roughly 500 ppb was estimated for this experimental configuration. Under dry fresh air purge (blue trace), we observed a moderate absorption on the order of 50%, whereas the curve without purge resulted in strong absorption lines going close to 90% of the maximum detector signal (violet trace). The corresponding CO_2 concentrations were 100 and 340 ppm, respectively. For the ambient air measurement, we noticed additional features at 2240–2285 cm^{-1}, which cannot be explained with the absorption lines of $^{12}C^{16}O_2$. A comparison with published spectra indicated that they are due to the P-branch absorption of the $^{13}C^{16}O_2$ isotope of carbondioxide. Its natural abundance of 1.11% is excellently confirmed by our experiments [8].

In order to make the absorption of the less abundant isotopomer better visible, human breath was exhaled into the purge tube of the FTIR. It is known from the literature that human breath can contain up to 4% or 40,000 ppm of CO_2 [5]. The lowest (red) trace of Fig. 4 shows the absorption spectrum of such a breath sample. There is now a large contribution of the $^{13}C^{16}O_2$ molecule absorption which interferes also strongly with the $^{12}C^{16}O_2$ band around 2300 cm^{-1}. Based on the previous experiments, we conclude that the $^{12}C^{16}O_2$ concentration was on the order of 5000 ppm, whereas 60 ppm was found for the $^{13}C^{16}O_2$; confirming again the natural abundance cited previously.

3.3 On-off measurement

We finally performed a quick practical test of this sensor system, during which the QCD was hooked up to a two-stage operational amplifier circuit instead of the low-noise Stanford amplifier. In addition, no spectral information was this time collected by the FTIR; thus revealing the integrated absorption signal only. As shown in Fig. 5, the purge was switched between dry and ambient air every 3 minutes, resulting in an amplified signal change on the order of 350 mV. Since this change corresponds to a concentration drop or increase of roughly 250 ppm, we can conservatively assign a sensitivity of 1.4 mV/ppm and a CO_2 detection limit of 20 ppm to the system. Although this performance might be useful for simple CO_2 level monitoring, it is evident that such integrated absorption measurements have limited wavelength selectivity only. However, a rough

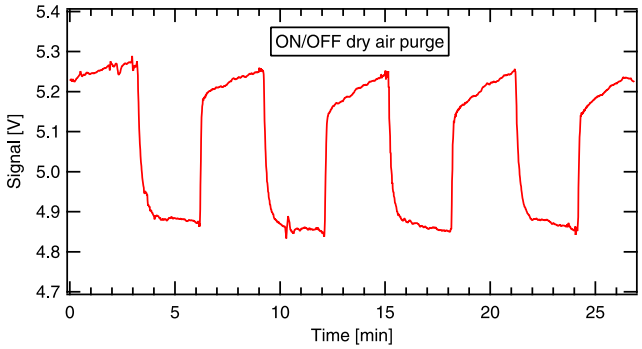

Fig. 5 On-off experiment using the glow-bar source, a QCD, and a two-stage operational amplifier circuit

estimation has shown that a compact diffraction spectrometer with 4 µm grating period, 100 mm working distance, and 100 µm slit width provides a resolution of 2 cm^{-1}, which would be by far sufficient to discriminate between the P- and R-branches of the two relevant CO_2 isotopomers.

4 Conclusion

In conclusion, we have shown a prototype CO_2 sensor which was operated with a blackbody source, a QCD, and an FTIR spectrometer. In a simplified experimental arrangement, amplification of the signal was accomplished with a two-stage operational amplifier circuit. We observed a detection limit of 500 ppb in the somewhat more sophisticated FTIR configuration, whereas the direct absorption measurement without spectral information resulted in roughly 20 ppm. Together with a suitable grating spectrometer, linear arrays of such QCDs will become very promising candidates for mid-infrared spectroscopic measurements in medical applications.

Acknowledgements The authors would like to acknowledge the Gebert-Ruef foundation for initiating this research and the nanotera initiative (project IRSENS) of the Swiss National Science Foundation for their generous support.

References

1. M. Beck, D. Hofstetter, T. Aellen, J. Faist, U. Oesterle, M. Ilegems, E. Gini, H. Melchior, Science **295**, 301 (2002)
2. N. Bandyopadyay, Y. Bai, B. Gokden, A. Myzaferi, S. Tsao, S. Slivken, M. Razeghi, Appl. Phys. Lett. **97**, 131117 (2010)
3. E. Israeli, Y. Ilan, S.B. Meir, C. Buenavida, E. Goldin, J. Clin. Gastroenterol. **37**, 139 (2003)
4. H. Sabana, T. Fritsch, M.B. Onana, O. Bouba, P. Hering, M. Murtz, Appl. Phys. B, Lasers Opt. **96**, 535 (2009)
5. M. Sowa, M. Murtz, P. Hering, J Breath Res **4**, 047101 (2010)
6. F.R. Giorgetta, E. Baumann, M. Graf, Q. Yang, C. Manz, K. Köhler, H.E. Beere, D.A. Ritchie, E. Linfield, A.G. Daveis, Y. Fedoryshyn, H. Jäckel, M. Fischer, J. Faist, D. Hofstetter, IEEE J. Quantum Electron. **45**, 1039 (2009)
7. See for instance http://www.spectralcalc.com/calc/spectralcalc.php
8. A. Kindness, I.L. Marr, Appl. Spectrosc. **51**, 17 (1997)